ACS APPLIED MATERIALS & INTERFACES

Letter

www.acsami.org

Direct Fabrication of the Graphene-Based Composite for Cancer Phototherapy through Graphite Exfoliation with a Photosensitizer

Gang Liu,[†] Hongmei Qin,[†] Tsukuru Amano,[‡] Takashi Murakami,[‡] and Naoki Komatsu*[,†]

[†]Graduate School of Human and Environmental Studies, Kyoto University, Sakyo-ku, Kyoto 606-8501, Japan

[‡]Department of Obstetrics and Gynecology, Shiga University of Medical Science, Seta, Otsu 520-2192, Japan

Supporting Information

ABSTRACT: We report on the application of pristine graphene as a drug carrier for phototherapy (PT). The loading of a photosensitizer, chlorin e6 (Ce6), was achieved simply by sonication of Ce6 and graphite in an aqueous solution. During the loading process, graphite was gradually exfoliated to graphene to give its composite with Ce6 (G−Ce6). This one-step approach is considered to be superior to the graphene oxide (GO)-based composites, which required pretreatment of graphite by strong oxidation. Additionally, the directly exfoliated graphene ensured a high drug loading capacity, 160 wt %, which is about 10 times larger than that of the functionalized GO. Furthermore, the Ce6 concentration for killing cells by G−Ce6 is 6−75 times less than that of the other Ce6 composites including GO−Ce6.

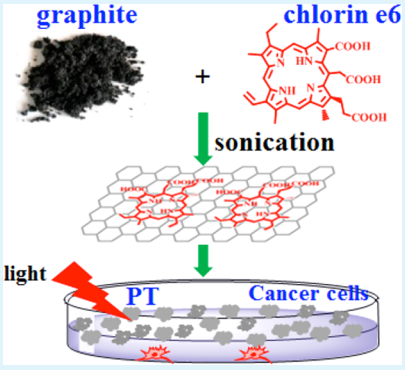

KEYWORDS: *graphene, photosensitizer, exfoliation, phototherapy, drug-delivery system*

Medicinal applications of nanomaterials, so-called "nanomedicine", have been attracting growing interest in recent years. Among various shapes of nanomaterials including nanotube and nanorod (1D),[1−3] nanosheet and a layered one (2D),[4−6] and nanosphere and nanoparticle (3D),[7−9] a 2D-layered nanosheet, most typically a few-layer graphene (FLG), has its own characteristics as a drug carrier: flat structure, hydrophobic surface, and large specific surface area.[10,11] Although it is advantageous to load anticancer drugs having flat structure and hydrophobic nature, the hydrophobicity prevents the carrier, such as FLG, from dispersing in a physiological environment. To solve this problem, the graphenes have been strongly oxidized to generate numerous hydrophilic oxygen-containing functional groups and employed as drug carriers.[5,10,12,13] Obviously, this chemical modification of graphenes, leading to graphene oxides (GOs), harms the planarity and hydrophobicity of the pristine graphenes, significantly decreasing the drug loading capacity and eventually losing the appeal of graphenes and 2D nanosheets as drug carriers.

On the other hand, phototherapy (PT), including photodynamic therapy (PDT) and photothermal therapy (PTT),[3,6,14−16] is a promising noninvasive treatment for cancer. To increase the efficacy of the therapy, the photosensitizer should be delivered to the lesion as selectively as possible, most likely with the aid of a carrier. It would be better if the loading capacity of the carrier is higher, as long as the composite has enough dispersibility in a physiological environment.

Herein, we report, for the first time, on a facile and convenient approach to fabricate the graphene-based composite with high drug loading efficiency and enough aqueous dispersibility directly from pristine graphite and a photosensitizer (chlorin e6, Ce6). The composite was well dispersed in a cell culture medium and directly applied to the cancer cell for PT. As a result, significant cytotoxicity was observed upon irradiation of light, while Ce6 without the graphene carrier was not cytotoxic irrespective of light irradiation. Ce6 is found to work not only as a photosensitizer in PT but also as an exfoliant and a dispersant for graphene. In addition, graphene in the composite plays an essential role as a carrier to deliver Ce6 into the cell.

The aqueous graphene dispersion was prepared by liquid-phase exfoliation,[17,18] which has been considered as a scalable and practical approach for the preparation of graphene. By using mild bath sonication, the pristine graphite was directly exfoliated to FLG in an aqueous solution with the aid of a photosensitizer, Ce6 (Figure 1a). A control experiment without Ce6 was also carried out under the same conditions. As shown in Figure 1b, blackish and colorless supernatants were obtained after centrifugation at 3000 rpm (1029*g*) for 1 h in the presence and absence of Ce6, respectively. The Ce6 composite with graphene (G−Ce6) exhibited good aqueous dispersibility, although both of the components, Ce6 and graphene, have poor or no solubility in water. The complexes of porphyrin- and pyrene-based host molecules, named nanotweezers[19−21] and nanocalipers,[22−24] with carbon nanotubes have shown similar

Received: August 11, 2015
Accepted: October 12, 2015
Published: October 12, 2015

DOI: 10.1021/acsami.5b07432
ACS Appl. Mater. Interfaces 2015, 7, 23402−23406

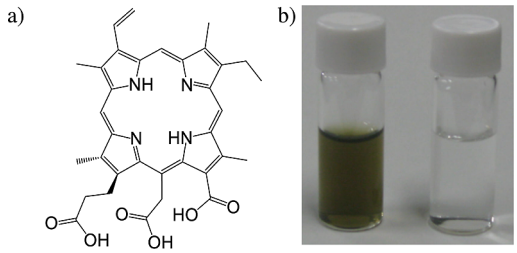

Figure 1. (a) Molecular structure of Ce6. (b) Pictures of supernatants after exfoliation and centrifugation in the presence (left) and absence (right) of Ce6 in water.

phenomena; the complex was dispersed well, despite low or no solubility of each component in methanol. The enhanced dispersibility through complexation can be attributed to the polarity induced by donation and acception of π electrons in the complex, as discussed in our previous papers.[21,25] The formation of an electron donor−acceptor complex is supported by quenching in the fluorescence spectrum, which will be shown below.

Typical atomic force microscopy (AFM) images of the greenish dispersion are shown in Figures 2 and S1. Most of the plates are 1.2−2.5 nm in thickness, proving that the exfoliated graphene has only a few layers. The plates observed in a scanning transmission electron microscopy (STEM) image (Figure S2) exhibit high transparency, supporting the above conclusion of thin graphene sheets. The graphene dispersion was further characterized by absorption, fluorescence, and Raman spectroscopies. In the absorption spectra (Figure 3a), the Q(I) band of free Ce6 at 655 nm disappeared after exfoliation and centrifugation, indicating almost no free Ce6 in the supernatant. This phenomenon can be explained by the poor solubility of Ce6 in water; that is, only the Ce6 complexed with graphene can be dissolved, and the free Ce6 was precipitated out during the centrifugation process. The large upward shift of the baseline and the red shift and broadening of the Soret and Q(I) bands of Ce6 indicate that a significant amount of graphene exists as a complex with Ce6 in the supernatant. This is supported by the fluorescence quenching observed in the fluorescence spectra (Figure 3b). To confirm the stability of the composite in water for longer duration, the dispersion was monitored by the absorption spectra after 1, 3, and 7 days (Figure S3). Although the absorbance gradually decreased for 7 days, no precipitation was observed for more than a month. This indicates that Ce6 works as a dispersant for graphene as well as an exfoliant for graphite.

Because the baseline shift and peak intensity correspond to the graphene and Ce6, respectively, in the absorption spectrum (Figure 3a), the loading capacity is calculated as 160 wt % (the detail is described in the Supporting Information). In this calculation, we used the absorption coefficient of each component, Ce6 (α_{Ce6} = 4910 mL mg^{-1} m^{-1} at 655 nm) and graphene ($\alpha_{graphene}$ = 3450 mL mg^{-1} m^{-1} at 660 nm), to estimate the weight ratio in the G−Ce6 composite. The capacity is 10 times larger than that using functionalized GO as a carrier.[6] The enhanced loading capacity can be attributed to a large flat area in the pristine graphene surface of the directly exfoliated graphene with Ce6. In contrast, GO has only a limited flat region to accept Ce6. The high Ce6 loading capacity in the composite is a remarkable advantage over the previously reported methods as well as the facile and direct approach in our process.

To clarify the structure, the exfoliated graphene was analyzed by Raman spectroscopy at the excitation wavelength of 488 nm. As shown in Figure 4a, typical Raman features of D, G, and 2D bands at 1356, 1577, and 2733 cm^{-1}, respectively, were observed for the pristine graphite. After exfoliation with Ce6, fluorescence overlapped with the Raman peaks, making the background of the exfoliated graphene upward. This phenomenon supports the existence of Ce6 with graphene.[26] After exfoliation, the 2D band in the Raman spectra shifts significantly from 2733 to 2708 cm^{-1} and the peak shape becomes much more symmetrical, indicating exfoliation of thin-layer graphene. This result is consistent with that of the AFM image in Figure 2. Another AFM and STEM observation of a much smaller lateral size of the graphene (Figures 2 and S1 and S2) than the graphite (more than 10 μm) is considered to correlate with the increased intensity in the Raman D band at 1356 cm^{-1} because of the large increase in the edges of the smaller size graphene.[27,28] The increase in the relative intensity of the D band may be attributed mainly to the edge rather than the defect because the I_D/I_G ratio of the exfoliated graphene (0.21) in Figure 4a is much smaller than those of the reduced GO (1.08−1.44).[29,30] The smaller I_D/I_G ratio secures a higher planarity of graphene, which did not disturb the $\pi-\pi$ stacking between the graphene and Ce6 and thus realized the high loading capacity mentioned above.

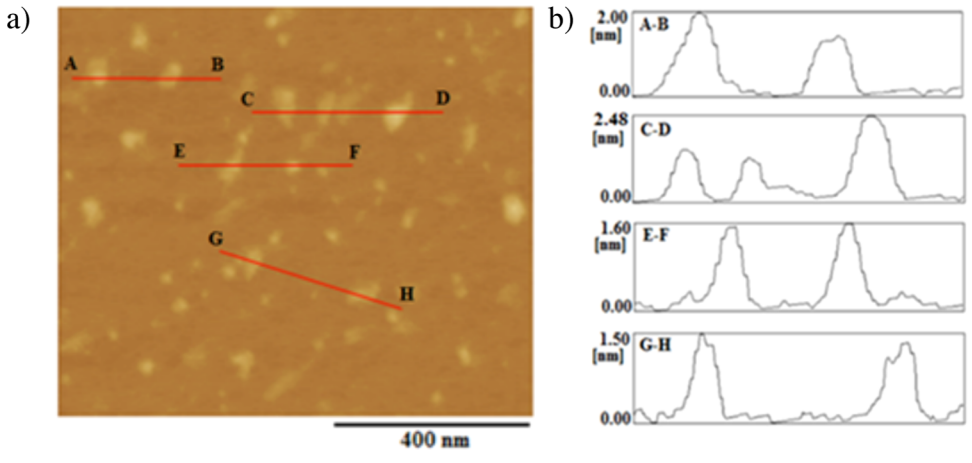

Figure 2. Typical AFM image (a) and height profiles (b) of the graphenes after exfoliation with Ce6.

DOI: 10.1021/acsami.5b07432
ACS Appl. Mater. Interfaces 2015, 7, 23402−23406

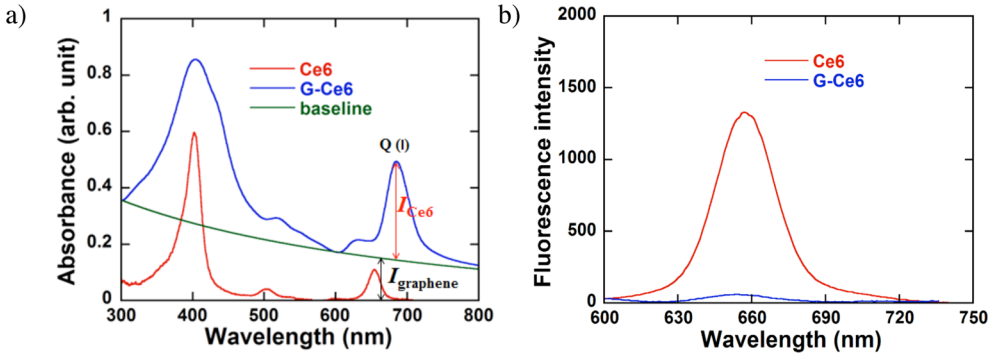

Figure 3. Absorption (a) and fluorescence (b; excited at 404 nm) spectra of Ce6 in water before and after exfoliation of graphene. The absorbance contributed by graphene is indicated as the baseline (green trace) in the absorption spectra (a). Red and black arrows indicate the absorbance of Ce6 at the Q(I) band and graphene at 660 nm, respectively.

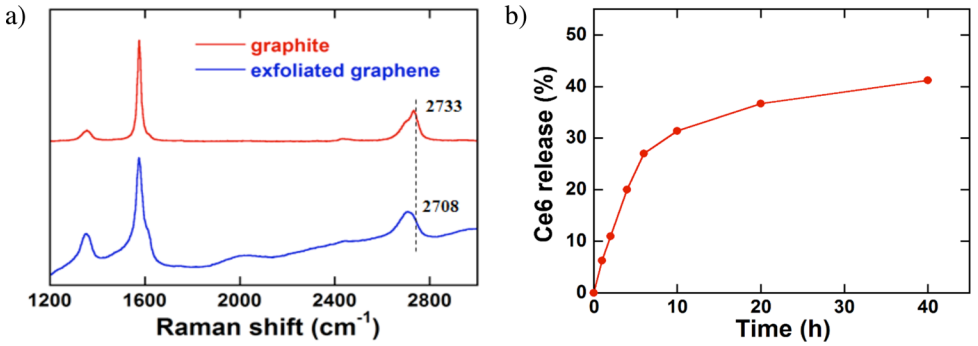

Figure 4. (a) Raman spectra of pristine graphite and exfoliated graphene at the laser wavelength of 488 nm. (b) Release profile of Ce6 from G−Ce6 in PBS at pH 7.4.

To apply the composite to cancer cells for PT, the aqueous medium was replaced by phosphate-buffered saline (PBS; pH 7.4). No absorption corresponding to free Ce6 was observed in the absorption spectrum after the medium exchange (Figure S5), indicating that the replacement of the medium did not cause decomplexation of G−Ce6. The PBS dispersion was quite stable without precipitation after a week (Figure S5). However, a drug release experiment through dialysis of the PBS dispersion of G−Ce6 against PBS (Supporting Information) revealed that Ce6 was released gradually (Figure 4b), although any precipitates were not observed.

The PBS dispersion of G−Ce6 was applied to HeLa cells with or without photoirradiation. The experiments using Ce6 instead of G−Ce6 were also carried out under the same conditions. Neither free Ce6 nor G−Ce6 exhibited any toxicity to HeLa cells in the dark at Ce6 concentrations of up to 0.20 μg mL^{-1} (Figure 5a). On the other hand, a remarkable difference in the cell viability was observed under light irradiation. While free Ce6 exhibited negligible cytotoxicity to HeLa cells up to 0.20 μg mL^{-1}, significant cytotoxicity was observed in the presence of G−Ce6 at Ce6 concentrations of more than 0.050 μg mL^{-1} (Figure 5b). More than 96% cancer cells were killed at Ce6 concentrations of more than 0.10 μg mL^{-1}. This concentration is 6−75 times less than that of other carriers such as GO,[6,31,32] lanthanide-doped nanoparticles,[33,34] conjugated polymers,[15] and other types of nanomaterials,[2,16] although some of the conditions such as the laser power and the kind of cancer cell are not the same. This indicates that Ce6 loaded on the graphene is delivered more efficiently into the cell. We could say that G−Ce6 is one of the best PT agents in terms of the drug loading capacity and cell killing efficiency as well as the facile and scalable preparation process.

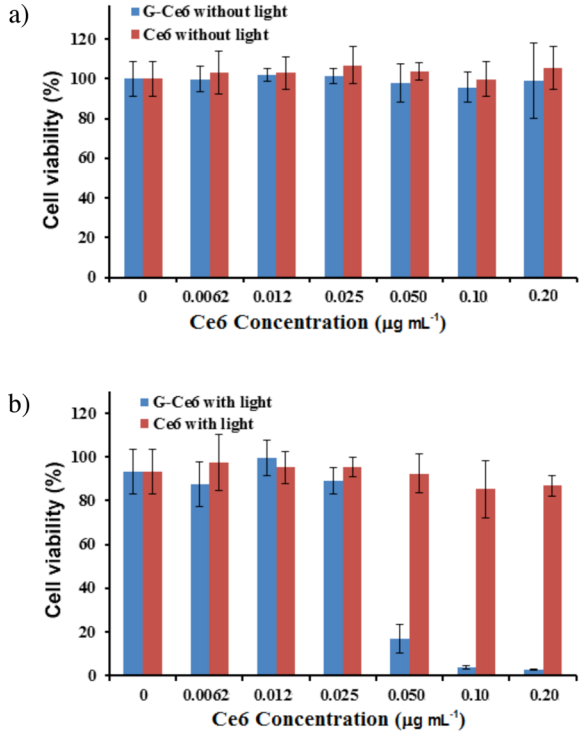

Figure 5. Cell viability of HeLa cells treated with G−Ce6 or Ce6 at various concentrations without (a) or with (b) irradiation of a 660 nm laser for 2 min. Error bars were based on four parallel measurements.

DOI: 10.1021/acsami.5b07432
ACS Appl. Mater. Interfaces 2015, 7, 23402−23406

The sharp contrast between G−Ce6 and Ce6 under light irradiation suggests an important role of graphene for this process. Therefore, the cellular uptake of Ce6 was evaluated by flow cytometry (FACS) of the HeLa cells treated with free Ce6 or G−Ce6 at concentrations of up to 0.20 μg mL^{-1} in the dark. Although the fluorescence intensities are proportional to the initial Ce6 concentration applied to the cells in both free Ce6 and G−Ce6 (Figure 6), the degree of increase in the fluorescence intensity is much larger in G−Ce6 than Ce6, indicating that Ce6 supported by graphene was uptaken by HeLa cells much more than free Ce6 at the same Ce6 concentration. In other words, graphene strongly accelerated insertion of the loaded drug into the cell. After being taken up as a composite, Ce6 is considered to be released according to the result of the release experiment (Figure 4b). Because the fluorescence of G−Ce6 was much weaker than that of Ce6 (Figure 3b), the origin of the fluorescence in FACS analysis (Figure 6) should be Ce6 released from G−Ce6 taken up by the cell (Figure 4b).

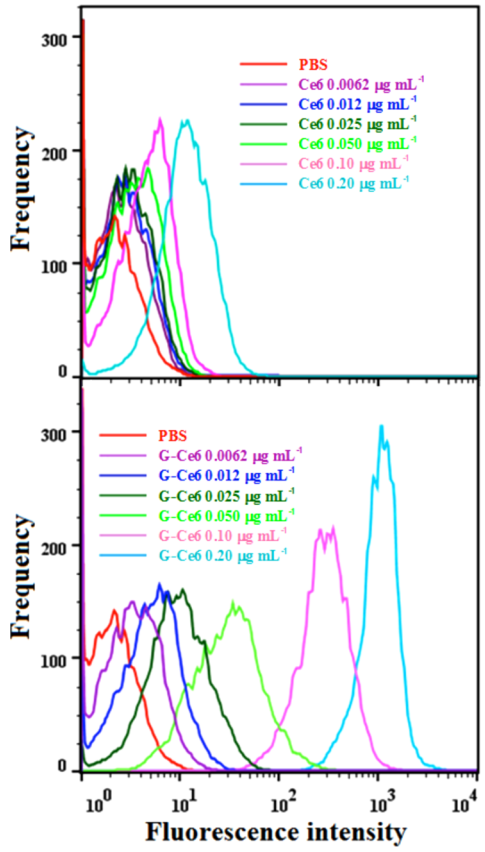

Figure 6. FACS analyses of HeLa cells after incubation with Ce6 and G−Ce6 at various Ce6 concentrations (0.0062−0.20 μg mL^{-1}) for 24 h.

When the 660 nm laser was irradiated at the cell taking up G−Ce6, Ce6 released from G−Ce6 inside the cell may generate reactive oxygen species (ROS) as the PDT agent because of the effective absorption of the 660 nm light, as shown in the red trace of Figure 3a. On the other hand, Ce6 in the G−Ce6 composite inside the cell could absorb the 660 nm light much less efficiently because of the red shift of the Q(I) band, as shown in the blue trace of Figure 3a, implying much less PDT effect of Ce6 in the composite. In fact, little generation of singlet oxygen, the main component of ROS to induce cell death, was confirmed from G−Ce6 upon irradiation of 660 nm light in the presence of 1,3-diphenylisobenzofuran, which is a well-known chemical probe of singlet oxygen (Figure S6). The absorption intensity difference between free Ce6 and complexed Ce6 at 660 nm indicates that Ce6 released from G−Ce6 works as a PDT agent to kill the cancer cells. In addition, graphene in G−Ce6 could absorb the 660 nm light. Once it absorbs the light, it gets excited and may return to the ground state by releasing heat. This implies that the photothermal effect may act as another factor to kill the cancer cells. Actually, a larger increase in the temperature was observed with G−Ce6 when the PBS solutions with and without G−Ce6 were exposed to light under the same conditions (0.8 °C increase with G−Ce6 compared with 0.4 °C without G−Ce6 in the Supporting Information). Therefore, the mechanism based on the very low cell viability in Figure 5b can be explained as PDT by Ce6 released from G−Ce6 as well as PTT by graphene complexed with Ce6.

In conclusion, we have fabricated a promising composite for PT through direct exfoliation of graphene from graphite with a photosensitizer, Ce6. Unexpectedly, the composite shows good dispersibility in a physiological environment without any chemical pretreatment of the graphene carrier and thus realizes a high drug loading efficiency. In addition, the loaded drug is efficiently inserted into the cell with the aid of a carrier, exerting the PT phenomenon in contrast to free Ce6. We believe that this approach of the direct fabrication of a graphene-based photosensitizer is widely applicable to the drug-delivery system based on a 2D-layered nanosheet.

■ ASSOCIATED CONTENT

Supporting Information

The Supporting Information is available free of charge on the ACS Publications website at DOI: 10.1021/acsami.5b07432.

Experimental details, materials and equipment, determination of the Ce6 loading capacity, and Figures S1−S6 (PDF)

■ AUTHOR INFORMATION

Corresponding Author

*E-mail: komatsu.naoki.7w@kyoto-u.ac.jp.

Author Contributions

All authors have given approval to the final version of the manuscript.

Notes

The authors declare no competing financial interest.

■ ACKNOWLEDGMENTS

This work was supported by a Grant-in-Aid for Scientific Research (B) (23350062) and a Grant-in-Aid for Japan Society for the Promotion of Science (JSPS) fellows (25-03339). G.L. acknowledges the JSPS for providing him with a postdoctoral fellowship (P13339).

■ REFERENCES

(1) Singh, S. R.; Vardharajula, S.; Ali, S. Z.; Tiwari, P. M.; Eroglu, E.; Vig, K.; Dennis, V. A. Functionalized Carbon Nanotubes: Biomedical Applications. *Int. J. Nanomed.* **2012**, *7*, 5361−5374.

(2) Huang, X.; Tian, X.-J.; Yang, W.-l.; Ehrenberg, B.; Chen, J.-Y. The Conjugates of Gold Nanorods and Chlorin e6 for Enhancing the

DOI: 10.1021/acsami.5b07432
ACS Appl. Mater. Interfaces 2015, 7, 23402−23406

Fluorescence Detection and Photodynamic Therapy of Cancers. *Phys. Chem. Chem. Phys.* **2013**, *15*, 15727−15733.
(3) Jang, B.; Park, J.-Y.; Tung, C.-H.; Kim, I.-H.; Choi, Y. Gold Nanorod−Photosensitizer Complex for Near-Infrared Fluorescence Imaging and Photodynamic/Photothermal Therapy In Vivo. *ACS Nano* **2011**, *5*, 1086−1094.
(4) Chung, C.; Kim, Y.-K.; Shin, D.; Ryoo, S.-R.; Hong, B. H.; Min, D.-H. Biomedical Applications of Graphene and Graphene Oxide. *Acc. Chem. Res.* **2013**, *46*, 2211−2224.
(5) Huang, P.; Xu, C.; Lin, J.; Wang, C.; Wang, X.; Zhang, C.; Zhou, X.; Guo, S.; Cui, D. Folic Acid-conjugated Graphene Oxide loaded with Photosensitizers for Targeting Photodynamic Therapy. *Theranostics* **2011**, *1*, 240−250.
(6) Tian, B.; Wang, C.; Zhang, S.; Feng, L.; Liu, Z. Photothermally Enhanced Photodynamic Therapy Delivered by Nano-Graphene Oxide. *ACS Nano* **2011**, *5* (9), 7000−7009.
(7) Choi, J.; Wang, N. S. In *Biomedical Engineering - From Theory to Applications*; Fazel-Rezai, R., Ed.; InTech: Rijeka, Croatia, 2011; pp 299−314.
(8) Zhao, L.; Chano, T.; Morikawa, S.; Saito, Y.; Shiino, A.; Shimizu, S.; Maeda, T.; Irie, T.; Aonuma, S.; Okabe, H.; Kimura, T.; Inubushi, T.; Komatsu, N. Hyperbranched Polyglycerol-Grafted Superparamagnetic Iron Oxide Nanoparticles: Synthesis, Characterization, Functionalization, Size Separation, Magnetic Properties, and Biological Applications. *Adv. Funct. Mater.* **2012**, *22*, 5107−5117.
(9) Lu, W.; Xiong, C.; Zhang, G.; Huang, Q.; Zhang, R.; Zhang, J. Z.; Li, C. Targeted Photothermal Ablation of Murine Melanomas with Melanocyte-Stimulating Hormone Analog−Conjugated Hollow Gold Nanospheres. *Clin. Cancer Res.* **2009**, *15*, 876−886.
(10) Pan, Y.; Sahoo, N. G.; Li, L. The Application of Graphene Oxide in Drug Delivery. *Expert Opin. Drug Delivery* **2012**, *9*, 1365−1376.
(11) Liu, J.; Cui, L.; Losic, D. Graphene and Graphene Oxide as New Nanocarriers for Drug Delivery Applications. *Acta Biomater.* **2013**, *9*, 9243−9257.
(12) Spinato, C.; Ménard-Moyon, C.; Bianco, A. In *Functionalization of Graphene*; Georgakilas, V., Ed.; Wiley-VCH Verlag GmbH & Co. KGaA: Weinheim, Germany, 2014; pp 95−138.
(13) Yang, K.; Wan, J.; Zhang, S.; Tian, B.; Zhang, Y.; Liu, Z. The Influence of Surface Chemistry and Size of Nanoscale Graphene Oxide on Photothermal Therapy of Cancer Using Ultra-Low Laser Power. *Biomaterials* **2012**, *33*, 2206−2214.
(14) Zhang, M.; Murakami, T.; Ajima, K.; Tsuchida, K.; Sandanayaka, A. S. D.; Ito, O.; Iijima, S.; Yudasaka, M. Fabrication of ZnPc/protein Nanohorns for Double Photodynamic and Hyperthermic Cancer Phototherapy. *Proc. Natl. Acad. Sci. U. S. A.* **2008**, *105*, 14773−14778.
(15) Gong, H.; Cheng, L.; Xiang, J.; Xu, H.; Feng, L.; Shi, X.; Liu, Z. Near-Infrared Absorbing Polymeric Nanoparticles as a Versatile Drug Carrier for Cancer Combination Therapy. *Adv. Funct. Mater.* **2013**, *23*, 6059−6067.
(16) Liu, T.; Wang, C.; Cui, W.; Gong, H.; Liang, C.; Shi, X.; Li, Z.; Sun, B.; Liu, Z. Combined Photothermal and Photodynamic Therapy Delivered by PEGylated MoS_2 Nanosheets. *Nanoscale* **2014**, *6*, 11219−11225.
(17) Ciesielski, A.; Samori, P. Graphene via Sonication Assisted Liquid-Phase Exfoliation. *Chem. Soc. Rev.* **2014**, *43*, 381−398.
(18) Du, W.; Jiang, X.; Zhu, L. From Graphite to Graphene: Direct Liquid-Phase Exfoliation of Graphite to Produce Single- and Few-Layered Pristine Graphene. *J. Mater. Chem. A* **2013**, *1*, 10592−10606.
(19) Peng, X.; Komatsu, N.; Bhattacharya, S.; Shimawaki, T.; Aonuma, S.; Kimura, T.; Osuka, A. Optically Active Single-Walled Carbon Nanotubes. *Nat. Nanotechnol.* **2007**, *2*, 361−365.
(20) Wang, F.; Matsuda, K.; Rahman, A. F. M. M.; Peng, X.; Kimura, T.; Komatsu, N. Simultaneous Discrimination of Handedness and Diameter of Single-Walled Carbon Nanotubes (SWNTs) with Chiral Diporphyrin Nanotweezers Leading to Enrichment of a Single Enantiomer of (6,5)-SWNTs. *J. Am. Chem. Soc.* **2010**, *132*, 10876−10881.
(21) Rahman, A. F. M. M.; Wang, F.; Matsuda, K.; Kimura, T.; Komatsu, N. Diameter-Based Separation of Single-Walled Carbon Nanotubes through Selective Extraction with Dipyrene Nanotweezers. *Chem. Sci.* **2011**, *2*, 862.
(22) Liu, G.; Wang, F.; Chaunchaiyakul, S.; Saito, Y.; Bauri, A. K.; Kimura, T.; Kuwahara, Y.; Komatsu, N. Simultaneous Discrimination of Diameter, Handedness, and Metallicity of Single-Walled Carbon Nanotubes with Chiral Diporphyrin Nanocalipers. *J. Am. Chem. Soc.* **2013**, *135*, 4805−4814.
(23) Liu, G.; Rahman, A. F. M. M.; Chaunchaiyakul, S.; Kimura, T.; Kuwahara, Y.; Komatsu, N. Bis(tert-butylpyrene) Nanotweezers and Nanocalipers: Enhanced Extraction and Recognition Abilities for Single-Walled Carbon Nanotubes. *Chem. - Eur. J.* **2013**, *19*, 16221−16230.
(24) Liu, G.; Saito, Y.; Nishio-Hamane, D.; Bauri, A. K.; Flahaut, E.; Kimura, T.; Komatsu, N. Structural Discrimination of Double-Walled Carbon Nanotubes by Chiral Diporphyrin Nanocalipers. *J. Mater. Chem. A* **2014**, *2*, 19067−19074.
(25) Peng, X.; Wang, F.; Kimura, T.; Komatsu, N.; Osuka, A. Optical Resolution and Diameter-Based Enrichment of Single-Walled Carbon Nanotubes through Simultaneous Recognition of Their Helicity and Diameter with Chiral Monoporphyrin. *J. Phys. Chem. C* **2009**, *113*, 9108−9113.
(26) Yang, H.; Hernandez, Y.; Schlierf, A.; Felten, A.; Eckmann, A.; Johal, S.; Louette, P.; Pireaux, J. J.; Feng, X.; Mullen, K.; Palermo, V.; Casiraghi, C. A Simple Method for Graphene Production Based on Exfoliation of Graphite in Water Using 1-Pyrenesulfonic Acid Sodium Salt. *Carbon* **2013**, *53*, 357−365.
(27) Casiraghi, C.; Hartschuh, A.; Qian, H.; Piscanec, S.; Georgi, C.; Fasoli, A.; Novoselov, K. S.; Basko, D. M.; Ferrari, A. C. Raman Spectroscopy of Graphene Edges. *Nano Lett.* **2009**, *9*, 1433−1441.
(28) Khan, U.; Porwal, H.; O'Neill, A.; Nawaz, K.; May, P.; Coleman, J. N. Solvent-Exfoliated Graphene at Extremely High Concentration. *Langmuir* **2011**, *27*, 9077−9082.
(29) Mohanty, N.; Nagaraja, A.; Armesto, J.; Berry, V. High-Throughput, Ultrafast Synthesis of Solution- Dispersed Graphene via a Facile Hydride Chemistry. *Small* **2010**, *6*, 226−231.
(30) Tung, V. C.; Allen, M. J.; Yang, Y.; Kaner, R. B. High-Throughput Solution Processing of Large-Scale Graphene. *Nat. Nanotechnol.* **2009**, *4*, 25−29.
(31) Cho, Y.; Choi, Y. Graphene Oxide-Photosensitizer Conjugate as a Redox-Responsive Theranostic Agent. *Chem. Commun.* **2012**, *48*, 9912−9914.
(32) Li, F.; Park, S.-J.; Ling, D.; Park, W.; Han, J. Y.; Na, K.; Char, K. Hyaluronic Acid-Conjugated Graphene Oxide/Photosensitizer Nanohybrids for Cancer Targeted Photodynamic Therapy. *J. Mater. Chem. B* **2013**, *1*, 1678−1686.
(33) Wang, C.; Cheng, L.; Liu, Y.; Wang, X.; Ma, X.; Deng, Z.; Li, Y.; Liu, Z. Imaging-Guided pH-Sensitive Photodynamic Therapy Using Charge Reversible Upconversion Nanoparticles under Near-Infrared Light. *Adv. Funct. Mater.* **2013**, *23*, 3077−3086.
(34) Wang, C.; Tao, H.; Cheng, L.; Liu, Z. Near-Infrared Light Induced in vivo Photodynamic Therapy of Cancer Based on Upconversion Nanoparticles. *Biomaterials* **2011**, *32*, 6145−6154.

DOI: 10.1021/acsami.5b07432
ACS Appl. Mater. Interfaces 2015, 7, 23402−23406